Synthesis of vanadium(III) complexes bearing iminopyrrolyl ligands and their role as thermal robust ethylene (co)polymerization catalysts

ARTICLE *in* DALTON TRANSACTIONS · FEBRUARY 2011

Impact Factor: 4.2 · DOI: 10.1039/c0dt01650k · Source: PubMed

4 AUTHORS, INCLUDING:

J. S. Mu
Ningbo University
10 PUBLICATIONS **71** CITATIONS
SEE PROFILE

Yue-Sheng Li
Chinese Academy of Sciences
116 PUBLICATIONS **2,113** CITATIONS
SEE PROFILE

Dalton Transactions

Cite this: *Dalton Trans.*, 2011, **40**, 3490

www.rsc.org/dalton

PAPER

Synthesis of vanadium(III) complexes bearing iminopyrrolyl ligands and their role as thermal robust ethylene (co)polymerization catalysts†

Jing-Shan Mu,[a,b] Yong-Xia Wang,[a] Bai-Xiang Li[a] and Yue-Sheng Li*[a]

Received 28th November 2010, Accepted 27th January 2011
DOI: 10.1039/c0dt01650k

Bis(imino)pyrrolyl vanadium(III) complexes **2a–e** [2,5-$C_4H_2N(CH{=}NR)_2$]$VCl_2(THF)_2$ [R = C_6H_5 (**2a**), 2,6-$Me_2C_6H_3$ (**2b**), 2,6-$^iPr_2C_6H_3$ (**2c**), 2,4,6-$Me_3C_6H_2$ (**2d**), C_6F_5 (**2e**)] and bis(iminopyrrolyl) vanadium(III) complex **4f** [$C_4H_3N(CH{=}N\text{-}2,6\text{-}^iPrC_6H_3)]_2VCl(THF)$ have been prepared in good yields from $VCl_3(THF)_3$ by treating with 1.0 and 2.0 equivalent deprotonated ligands in tetrahydrofuran (THF), respectively. These complexes were characterized by FTIR and mass spectra as well as elemental analysis. Structures of **2c** and **4f** were further confirmed by X-ray crystallographic analysis. DFT calculations indicated the configurations of **2a–e** with two nitrogen atoms of the chelating ligand coordinating with vanadium metal centre were more stable in energy. These complexes were employed as catalysts for ethylene polymerization at various reaction conditions. On activation with Et_2AlCl, these complexes exhibited high catalytic activities (up to 22.2 kg $mmol^{-1}{}_V$ h^{-1} bar^{-1}) even at high temperature, suggesting these catalysts possessed remarkable thermal stability. Moreover, high molecular weight polymer with unimodal molecular weight distributions can be obtained, indicating the polymerization took place in a single-site nature. The copolymerizations of ethylene and 1-hexene with precatalysts **2a–e** and **4f** were also explored in the presence of Et_2AlCl. Catalytic activity, comonomer incorporation, and properties of the resultant polymers can be controlled over a wide range by tuning catalyst structures and reaction parameters.

Introduction

Among the transition metals complexes, vanadium-based catalysts have played a critically important role in producing high molecular weight polyethylene with narrow molecular weight distribution as well as ethylene/α-olefin or functional α-olefin copolymers with high comonomer incorporations.[1] However, catalyst deactivation at high polymerization temperature is an issue in polymerization with vanadium(III) complexes due to reduction of catalytically active vanadium species to low-valent, less active or inactive species. Therefore, the design and synthesis of new vanadium(III) complexes with high thermal stability in olefin polymerizations have attracted considerable attention.[2–8]

Nitrogen-based polydentate ligands have been widely used in olefin polymerization catalysis over the past decades. A key attraction of these ligands is their availability and amenability to modification *via* straightforward Schiff-base condensation procedures.[9–17] We became attracted to building on this platform to prepare efficient vanadium metal catalysts for precise, controlled olefin polymerization. Recently, we reported a series of vanadium(III) complexes bearing β-enaminoketonato[18a–d] and salicyladiminato[18c–f] ligands, which were active towards ethylene (co)polymerization in the presence of alkylaluminium compounds and produced high molecular weight (co)polymers. More recently, we introduced a new family of vanadium(III) containing mono(iminopyrrolyl) ligands.[19] These complexes were also efficient catalysts for ethylene polymerization. However, at high polymerization temperature, broad molecular weight distribution polymers were obtained since the fast deactivation or chain transfer to aluminium occurred. Thus, this work was initially aimed at introducing the steric bulk around the mental center to stabilize vanadium(III) complexes and improve the thermal stability.

In this paper, we described the synthesis and characterization of new vanadium(III) complexes bearing bis(imino)pyrrolyl ligands **2a–e** and bis(iminopyrrolyl) chelate ligand **4f** (see Scheme 1), and explored the potential application in ethylene polymerization and the copolymerization of ethylene with 1-hexene. As expected, these new precatalysts could effectively restrain active vanadium center from deactivation and control chain transfer reaction, therefore, high molecular weight polymers with unimodal molecular weight distributions can be easily obtained at high temperature.

[a]*State Key Laboratory of Polymer Physics and Chemistry, Changchun Institute of Applied Chemistry, Chinese Academy of Sciences, Changchun, 130022, China. E-mail: ysli@ciac.jl.cn; Fax: +86-431-85262039*
[b]*Graduate School of the Chinese Academy of Sciences, Changchun Branch, Changchun, 130022, China*

† CCDC reference numbers 802187–802188. For crystallographic data in CIF or other electronic format see DOI: 10.1039/c0dt01650k

Table 1 Crystallographic data and collection parameters, and refinement parameters

	2c	4f
Empirical formula	$C_{38}H_{54}Cl_2N_3O_2V$	$C_{38}H_{50}ClN_4OV$
fw	706.68	665.21
Temperature	185(2) K	185(2) K
Cryst. syst.	Triclinic	Monoclinic
Space group	$P\bar{1}$	$C2/c$
a/Å	9.3696(7)	11.0190(9)
b/Å	15.8826(12)	14.8900(12)
c/Å	16.5052(13)	22.0694(18)
V/Å^3	2345.1(3)	3534.5(5)
α (°)	95.5610(10)	90
β (°)	106.3050(10)	102.5500(10)
γ (°)	90.2220(10)	90
Z	2	4
D_{calc}/Mg m^3	1.001	1.250
Abs. coeff./mm^{-1}	0.354	0.391
F(000)	752	1416
Crystal size/mm	0.32 × 0.17 × 0.11	0.24 × 0.18 × 0.08
θ range (deg)	1.29 to 26.04	1.89 to 26.03
Reflections collected/unique	13264/9045 [R_{int} = 0.0217]	9803/3489 [R_{int} = 0.0254]
Abs. Corr.	Semi-empirical from equivalents	Semi-empirical from equivalents
Max. and min. transmn	0.9621 and 0.8952	0.9709 and 0.9109
Refinement method	Full-matrix least-squares on F^2	Full-matrix least-squares on F^{s2}
Final R indices [$I > 2\sigma(I)$]	R_1 = 0.0492, wR_2 = 0.1194	R_1 = 0.0513, wR_2 = 0.1405
R indices (all data)	R_1 = 0.0706, wR_2 = 0.1289	R_1 = 0.0594, wR_2 = 0.1464
Largest diff. peak and hole/Å^{-3}	0.339 and –0.337 e	1.008 and –0.435 e

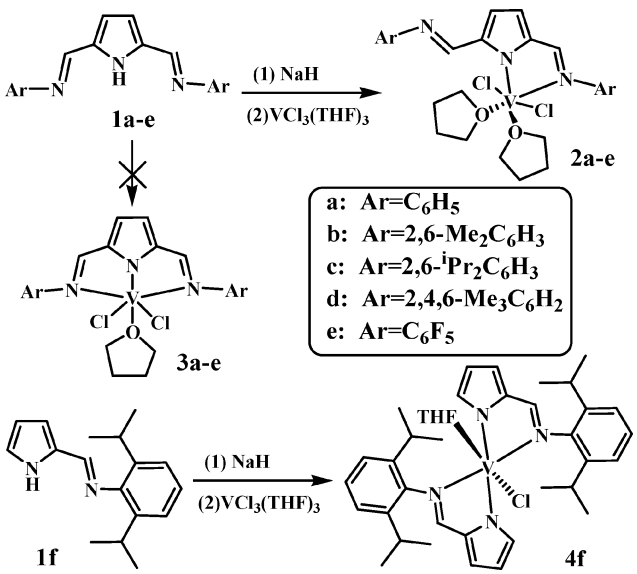

Scheme 1 General synthetic route of vanadium(III) complexes **2a–e** and **4f**.

Results and discussion

Synthesis and characterization of iminopyrrolyl vanadium(III) complexes (2a–f)

A general synthetic route of new bis(imino)pyrrolyl vanadium complexes used in this study is shown in Scheme 1. The bis(imino)pyrrolyl ligands **1a–e** and bis(iminopyrrolyl) chelate ligand **1f** were deprotonated by 1.0 equiv. of NaH, followed by treating with $VCl_3(THF)_3$ in THF at room temperature. Then the pure complexes **2a–e** and **4f** were isolated by recrystallization from a mixture of THF and hexane at room temperature. The mono(iminopyrrolyl) vanadium(III) complex [C_4H_2N(CH=N-2,6-^{i}PrC_6H_3)]$VCl_2(THF)_2$ (**I**) was also synthesized for comparison.[19] These complexes were identified by FTIR and mass spectra as well as elemental analysis. The severe line broadening in the ^{1}H NMR spectra indicates that these complexes are paramagnetic species.[18]

Crystals of **2a–e** and **4f** suitable for crystallographic analysis were grown from the chilled concentrated THF–hexane mixture solution. The ratio of THF–hexane was adjusted in the range of 1 : 1 to 1 : 3, according to the solubility of the complex. A dark red block microcrystal of **2c** and **4f** suitable for X-ray crystallographic analysis was grown from the chilled concentrated THF–hexane mixture solution. The crystallographic data together with the collection and refinement parameters are summarized in Table 1. Molecular structures for **2c** and **4f** are shown in Fig. 1 and 2.

Complexes **2c** and **4f** fold six-coordinate distorted octahedral geometry around the V metal center, which are similar to mono(iminopyrrolyl) complex **I**.[19] In complex **2c**, the equatorial positions are occupied by nitrogen and chlorine atoms of the chelating bis(imino)pyrrolyl ligand, and two additional oxygen atoms of two THF molecules are coordinated on the axial position (Fig. 1). However, one nitrogen atom of imino-nitrogen coordinates to vanadium, another one bents away from the metal center, which is somewhat analogous to that [2,5-C_4H_2NH(CH=N-2,6-iPrC_6H_3)$_2$]Zr$(NMe_2)_3$ reported by Bochmann.[17] Compared with complex **I**, **4f** showed a small but significant lengthening in the V–N(1) bond distance (**4f**, 2.0483(19) Å; **I**, 2.037(3) Å) since the two coordinated ligands repulsed each other (Fig. 2).

As shown in Scheme 2, density functional theory (DFT) calculations indicated that extra energies of 4.4–15.8 kcal mol^{-1} were needed for complexes **2a–e** to dissociate into **3a–e** and THF. Thus, the configurations with two nitrogen atoms of the

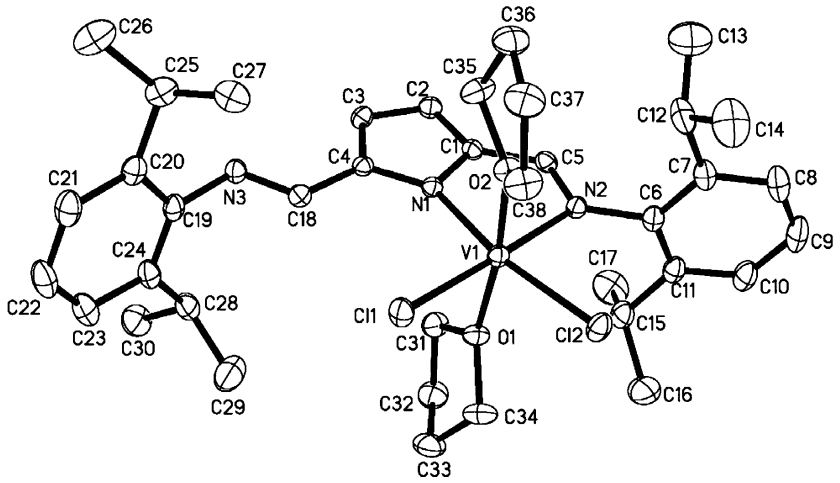

Fig. 1 Molecular structure of complex **2c**. Thermal ellipsoids are drawn at the 30% probability level, and H atoms are omitted for clarity. Selected bond distances (Å) and bond angles (°): V(1)–O(2), 2.0462(15); V(1)–N(1), 2.1012(19); V(1)–O(1), 2.0543(15); V(1)–N(2), 2.1646(18); V(1)–Cl(1), 2.3450(7); V(1)–Cl(2), 2.3225(7); O(2)–V(1)–N(1), 88.64(7); O(2)–V(1)–O(1), 172.79(7); N(1)–V(1)–O(1), 87.38(7); O(2)–V(1)–N(2), 93.82(7); N(1)–V(1)–N(2), 78.65(7); O(1)–V(1)–N(2), 91.28(7); O(2)–V(1)–Cl(1), 88.21(5); N(1)–V(1)–Cl(1), 98.24(5); O(1)–V(1)–Cl(1), 86.42(5); N(2)–V(1)–Cl(1), 176.23(5); O(2)–V(1)–Cl(2), 93.93(5); N(1)–V(1)–Cl(2), 165.75(5); O(1)–V(1)–Cl(2), 91.40(5); N(2)–V(1)–Cl(2), 87.19(5); Cl(1)–V(1)–Cl(2), 95.85(3).

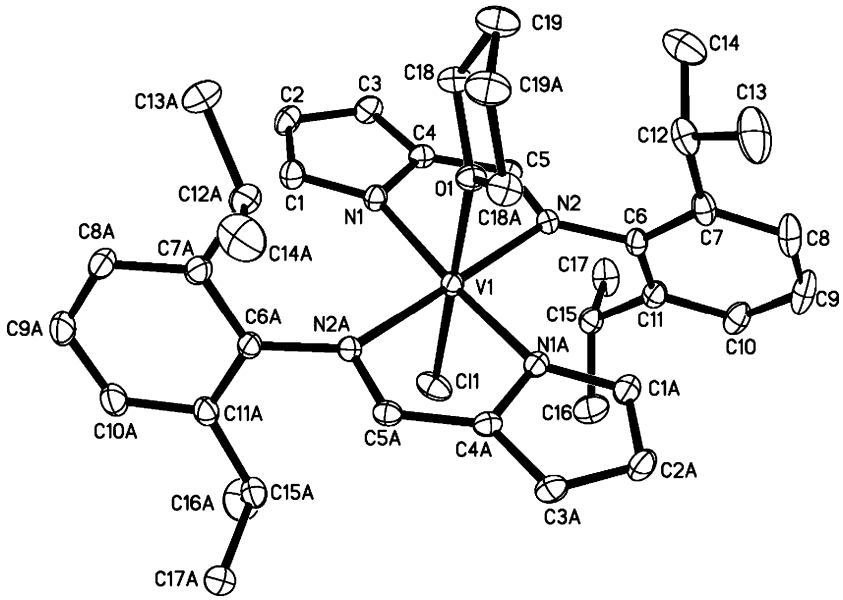

Fig. 2 Molecular structure of complex **4f**. Thermal ellipsoids are drawn at the 30% probability level, and H atoms are omitted for clarity. Selected bond distances (Å) and bond angles (°):V(1)–N(1), 2.0483(19); V(1)–N(1)A, 2.0483(19); V(1)–O(1), 2.135(2); V(1)–N(2), 2.1697(19); V(1)–N(2)A, 2.1697(19); V(1)–Cl(1), 2.2671(10); N(1)–V(1)–N(1)A, 173.40(11); N(1)–V(1)–O(1), 86.70(6); N(1)A–V(1)–O(1), 86.70(6); N(1)–V(1)–N(2), 79.62(7); N(1)A–V(1)–N(2), 100.31(7); O(1)–V(1)–N(2), 89.34(5); N(1)–V(1)–N(2)A, 100.31(7); N(1)A–V(1)–N(2)A, 79.61(7); O(1)–V(1)–N(2)A, 89.34(5); N(2)–V(1)–N(2)A, 178.68(10); N(1)–V(1)–Cl(1), 93.30(6); N(1)A–V(1)–Cl(1), 93.30(6); O(1)–V(1)–Cl(1), 180.0; N(2)–V(1)–Cl(1), 90.66(5); N(2)A–V(1)–Cl(1), 90.66(5).

potentially tridentate ligands coordinating with vanadium metal centre are much more stable in energy. The theory calculations results were in accordance with X-ray crystallographic analysis.

Ethylene polymerization catalyzed by new vanadium complexes

The bis(imino)pyrrolyl ligands act as a bidentate rather than tridentate ligand, which is different form the structures of initial design; nevertheless, complexes **2a–e** have been investigated as thermal stability ethylene polymerization catalysts in the presence of Et_2AlCl and promoter $Cl_3CCOOEt$,[25] as shown in Table 2. All these complexes **2a–e** and **4f** exhibited notable catalytic activities for ethylene polymerization, and the polymers prepared were linear polyethylene confirmed by ^{13}C NMR spectra and possessed relatively high molecular weights with unimodal molecular weight distributions confirmed by GPC.

The substituent in the ligands and reaction temperature considerably influence polymerization behaviors. As shown in Fig. 3, complexes **2a–e** exhibited a temperature-dependence of catalytic activity with a maximum at about 50 °C. Notably,

Table 2 Ethylene polymerization catalyzed by **2a–e** and **4f**[a]

Entry	Catalyst	Al/V (molar ratio)	T/°C	Yield/g	Activity[b]	M_w[c]/10^4	M_w/M_n[c]
1	**2a**	4000	50	0.47	28.2	4.55	2.00
2	**2b**	4000	50	0.59	35.4	5.03	2.03
3	**2c**	4000	25	0.44	26.4	12.4	2.28
4	**2c**	4000	50	0.56	33.6	6.03	2.10
5	**2c**	4000	75	0.37	22.2	1.33	1.91
6	**2c**	2000	50	0.33	19.8	8.84	2.20
7	**2c**	6000	50	0.57	34.2	4.46	1.99
8[d]	**2c**	4000	50	0.75	30.0	7.66	2.22
9[e]	**2c**	4000	50	1.41	28.2	9.08	2.18
10	**2d**	4000	50	0.32	19.2	4.94	1.98
11	**2e**	4000	50	0.36	21.6	3.64	2.04
12	**4f**	4000	50	0.21	12.6	6.23	1.87
13	**I**	4000	50	0.65	39.0	3.36	1.80

[a] Reaction conditions: 0.2 μmol catalyst, ETA/V (molar ratio) = 500, V_{total} = 50 mL, 1 atm ethylene pressure, in toluene for 5 min. [b] Activity in kg mmolv^{-1} h^{-1}. [c] Determined by GPC in 1,2,4-trichlorobenzene *versus* polystyrene standard. [d] 0.1 μmol catalyst, 15 min. [e] 0.1 μmol catalyst, 30 min.

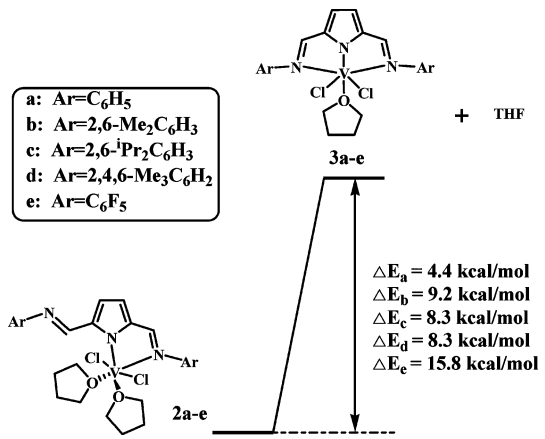

Scheme 2 DFT calculation results.

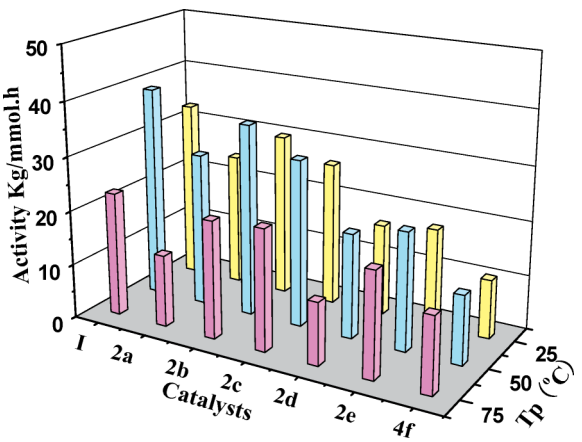

Fig. 3 Effects of ligand structures on activities of catalysts **2a–e** and **4f** from 25 °C to 75 °C. Reaction conditions: 0.2 μmol of catalyst, ETA/V (molar ratio) = 500, Al/V (molar ratio) = 4000, V_{total} = 50 mL, 1 atm ethylene pressure, in toluene for 5 min.

bis(iminopyrrolyl) complex **4f** shows the highest activity at 75 °C, maybe due to the deactivation of the bimolecular species being hindered by the steric hindrance. The selection of the substituent at imine nitrogen in the ligands sensitively affected not only the activity for ethylene polymerization but also the thermal stability of complexes. The catalytic activity ratio of 75 °C to 50 °C (A_{75}/A_{50}) was monitored to describe the thermal stability of catalysts. Just as expected, the value of A_{75}/A_{50} was improved from 0.48 (**2a**) to 0.61 (**2b**) and 0.72 (**2c**) with increasing of the steric hindrance. In combination with electron withdrawing groups as **2e**, the effect of five fluorine groups at imine group became remarkable and the activities changed slightly with increasing polymerization temperature (A_{75}/A_{50} = 0.88). Compared with bis(imino)pyrrolyl complexes **2a–e**, bis(iminopyrrolyl) complex **4f** displayed the better thermal stability, which is in accordance with the highest value of A_{75}/A_{50} (1.06). In addition, although the catalytic activity of **I** was higher than that of complexes **2c** and **4f** at lower temperature, the A_{75}/A_{50} values of **2c** (0.72) and **4f** (1.06) are much higher than that of **I** (0.58), indicating the notable stability of **2c** and **4f** than **I**. It can be seen from the above results that electronic withdrawing and steric effects were beneficial to improve the thermal stability of catalysts.

The molecular weight and molecular weight distributions were considerably influenced by the substituent in ligands and reaction temperature. The molecular weights were enhanced with increasing the steric hindrance of ligands (**4f** > **2c** > **2d**, **2b** > **2a**, **2e** > **I**) (see Table 2), indicating that the chain transfer reactions were hindered due to the protection of steric hindrance. In addition, although the molecular weights of the polymers decreased at high reaction temperature, the molecular weight distributions were kept in the range of 1.78–2.38, suggesting the characteristics of single-site catalysts. As a comparison, the molecular weight distributions of **I** was seriously broadened with increasing the temperature due to some deactivation (see Fig. 4).

The polymerization reactions carried out with different Al/V molar ratios by **2c** are listed in Table 2. The increase in Al/V ratio from 2000 to 6000 caused change either in the catalytic activity or the molecular weights for the resultant polymers. These results suggested that the dominant chain-transfer pathway was chain-transfer to aluminium alkyls under these conditions (entries 4, 6 and 7 in Table 2). To investigate the catalytic lifetime of complex **2c**, ethylene polymerizations were conducted for 5, 15, and 30 min at 50 °C (entries 4, 8 and 9 in Table 2). The relationship between the polymerization time and the polymer yield indicates that the **2c**/Et_2AlCl catalyst has a catalytic lifetime of at least 30 min.

Table 3 Ethylene/1-hexene copolymerizations with different complex/Et_2AlCl systems[a]

Entry	Catalyst	1-Hexene/mol L^{-1}	T/°C	Yield/g	Activity/kg $mmol_v^{-1}$ h^{-1}	Hexene incorp.	M_w[b]/10^3	M_w/M_n[b]	T_m[c]/°C
1	**2a**	0.2	25	0.20	4.80	4.20	25.9	1.86	114.6
2	**2b**	0.2	25	0.29	6.96	3.88	37.3	1.87	115.8
3[d]	**2c**	0.2	25	0.18	4.32	3.10	155.2	3.88	117.4
4[e]	**2c**	0.2	25	0.22	5.28	3.00	50.2	1.82	117.1
5	**2c**	0.2	25	0.31	7.44	3.04	45.1	1.81	117.6
6	**2c**	0.6	25	0.21	5.04	8.80	20.7	1.76	100.7
7	**2c**	0.6	50	0.75	5.63	9.80	8.6	1.89	76.8
8	**2c**	0.6	75	0.45	3.38	16.1	3.2	1.80	—
9	**2d**	0.2	25	0.17	4.08	3.64	24.8	1.84	115.8
10	**2e**	0.2	25	0.23	5.52	2.22	26.1	1.90	120.1
11	**4f**	0.2	25	0.10	2.40	2.00	45.8	2.06	122.3
12	**I**	0.2	25	0.32	7.68	3.45	28.6	1.89	116.8

[a] Reaction conditions: 0.5 μmol catalyst, Al/V (molar ratio) = 4000, ETA/V (molar ratio) = 500, V_{total} = 50 mL, 1 atm ethylene pressure, in toluene polymerization for 5 min. [b] Weight-average molecular weight determined by GPC in 1,2,4-trichlorobenzene *versus* polystyrene standard. [c] Determined by DSC. [d] Al/V (molar ratio) = 500. [e] Al/V (molar ratio) = 2000.

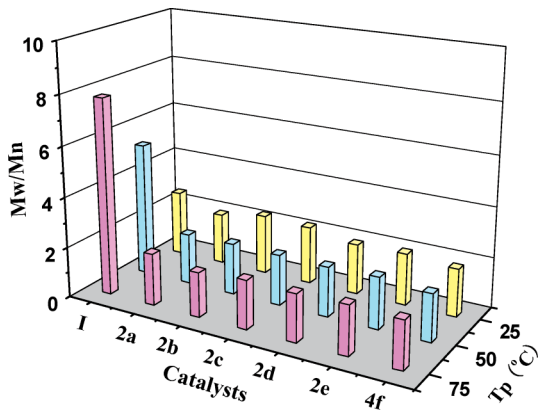

Fig. 4 Effect of ligands structures on molecular weight distributions from 25 °C to 75 °C. Reaction conditions: Reaction conditions: 0.2 μmol of catalyst, ETA/V (molar ratio) = 500, Al/V (molar ratio) = 2000, V_{total} = 50 mL, 1 atm ethylene pressure, in toluene for 5 min.

Ethylene/1-hexene copolymerization catalyzed by new vanadium complexes

The copolymerizations of ethylene/1-hexene were also studied and the representative results are summarized in Table 3. In the presence of cocatalyst Et_2AlCl and promoter $Cl_3CCOOEt$, catalysts **2a–e** and **4f** show highly activities towards ethylene/1-hexene copolymerization and produce copolymers with high molecular weight and unimodal molecular weight distributions. The ^{13}C and ^{1}H NMR spectroscopy revealed that the signals belonging to chain-end double bonds were not detected for low molecular weight copolymers, indicating that chain transfer to aluminium was the dominant chain-transfer pathway under these reaction conditions. Both the catalytic activity and the molecular weight were dependent upon the Al/V molar ratio employed, the highest catalytic activity appeared when the Al/V (mol/mol) equals *ca.* 4000 for **2c**/Et_2AlCl catalyst system, whereas the molecular weights of the resultant copolymers decreases sharply with the increase of Al/V molar ratio (entries 3–5), indicating chain transferred reaction to Al occurring. In addition, the molecular weight distribution of the resultant polymers also decreased with the increase of Et_2AlCl dosage (PDI = 3.88, Al/V = 500; PDI = 1.81, Al/V = 4000). A significant increase in 1-hexene incorporation of **2c**/Et_2AlCl system was found if the copolymerization was conducted at high temperature and high 1-hexene initial concentration (entries 6–8 in Table 3). The level of 1-hexene incorporation can approach 16 mol% in the resultant copolymer. Although the molecular weights of the resultant copolymers decreased with temperature or 1-hexene concentration, the molecular weight distributions remained constant, indicating a single-site catalytic behavior. Complex **4f** show much lower catalytic activity and the 1-hexene incorporations (*ca.* 2.0%) than **2a–e** towards ethylene/1-hexene copolymerization. Compared with complex **I**, analogues **2c** and **4f** offered much high molecular weights copolymers under the same polymerization conditions.

The microstructures of ethylene/1-hexene copolymers are established by ^{13}C NMR in *o*-$C_6D_4Cl_2$ at 135 °C, with the assignment of the microstructure following previous work reported by Hsieh and Randall.[20] As shown in Fig. 5, the resultant copolymer possessed isolated 1-hexene inserted unit ([EHE] assigned as $T_{\delta\delta}$) among the repeated ethylene insertions, and the alternating sequence ([HEH] assigned as $S_{\beta\beta}$) was also present with a low extent. The resonances ascribed to two 1-hexene repeating unit ([EHH] $T_{\beta\delta}$) were seen in the spectrum, but no peaks due to block-type sequence of 1-hexene repeating units were observed even with 16.1 mol% comonomer incorporation (assigned as $S_{\alpha\alpha}$). In addition, a trace amount of resonances due to so-called pseudo random ($S_{\alpha\beta}$, $S_{\beta\gamma}$ and $T_{\gamma\delta}$) sequences was present.

The triad distributions data and reactivity ratios r_e and r_h for each catalyst were calculated at 50 °C according to ^{13}C NMR using the method of Hsieh and Randall,[20] as shown in Table 4. The steric hindrance and electron effect of the ligands exerted obvious influence on the value of r_e, which manifested as the capability of incorporation of 1-hexene. For complexes **2a–d** containing electron donating imino groups, the 1-hexene selectivity increases in the order of decreasing steric bulk at the 2,6-aryl positions, *i*Pr < Me < H (**2c** < **2b**, **2d** < **2a**, respectively) at the same feed ratio of comonomers. Specifically, the r_e values of these complexes decreased, while r_h values increased from *i*Pr to H

Table 4 Triad distributions and reactivity ratios for ethylene/1-hexene copolymerization

Entry	Cat.	$[H]_{feed}$	$[H]_{copolymer}$	Triads						r_e	r_h
				[EHE]	[EHH]	[HHH]	[HEH]	[HEE]	[EEE]		
1	**2a**	0.677	0.057	0.037	0.020	0.000	0.000	0.094	0.849	40.2	0.10
2	**2b**	0.677	0.052	0.035	0.017	0.000	0.000	0.088	0.860	43.2	0.09
3	**2c**	0.677	0.039	0.036	0.003	0.000	0.000	0.076	0.885	50.5	0.02
4	**2d**	0.677	0.046	0.037	0.010	0.000	0.000	0.083	0.870	46.0	0.06
5	**2e**	0.677	0.031	0.030	0.001	0.000	0.000	0.061	0.909	64.1	0.01
6	**4f**	0.677	0.033	0.027	0.006	0.000	0.000	0.061	0.906	64.7	0.05
7	**I**	0.677	0.054	0.036	0.018	0.000	0.000	0.090	0.856	42.2	0.09

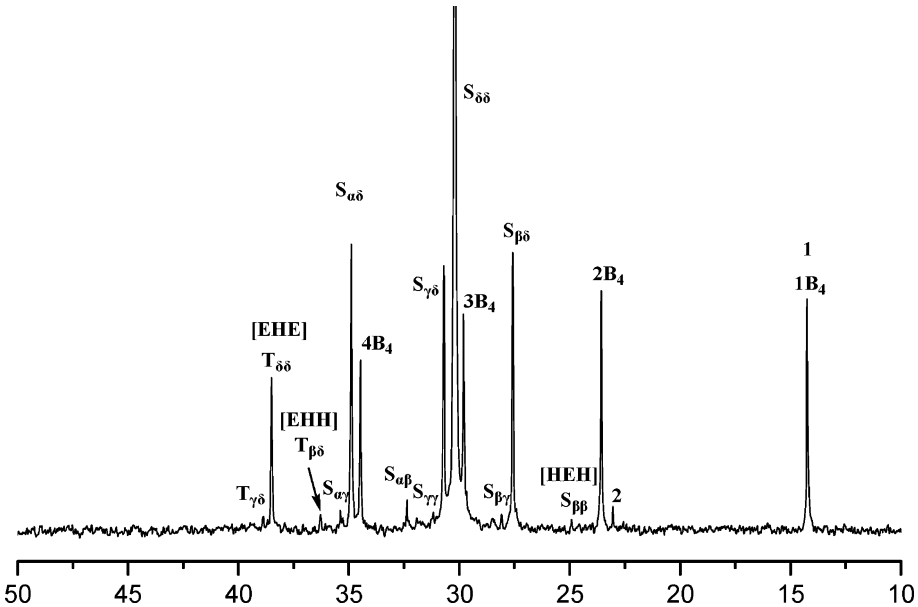

Fig. 5 The typical ^{13}C NMR spectra for poly(ethylene-*co*-1-hexene)s obtained by catalyst **2c**.

substituents. The influence of the electronic withdrawing effects on 1-hexene selectivity was investigated by comparison of the copolymerization behavior of complexes **2a** and **2e**. Compared to complex **2a** ($r_h = 0.10$, $r_e = 40.2$), complex **2e** showed a much higher tendency to incorporate ethylene ($r_e = 64.1$), and lower tendency to incorporate 1-hexene ($r_h = 0.01$). However, the coordination and insertion velocity of 1-hexene by complex **I** was relatively higher than complexes **4f** and **2c**. This was manifested in the higher value of r_e and lower values of r_h for **2c** ($r_e = 50.5$, $r_h = 0.02$) and **4f** ($r_e = 64.7$, $r_h = 0.05$) compared with those for **I** ($r_e = 42.2$, $r_h = 0.09$).

Conclusion

In summary, we have prepared and characterized a series of vanadium(III) complexes bearing iminopyrrolyl ligands (**2a–e** and **4f**). These complexes displayed promising thermal stability and high activity towards ethylene polymerization in the presented of Et_2AlCl as a cocatalyst and $Cl_3CCOOEt$ as reactivation reagent even at high temperature. The resultant polymers possessed high molecular weights with unimodal distributions, strongly suggesting that these polymerizations proceeded with a single catalytically active species. Especially, the thermal stability was improved with increasing the steric hindrance effect and electron withdrawing effect in N-aryl moiety of the ligands.

In addition, these complexes also exhibited high catalytic activity for ethylene/1-hexene copolymerization. Changing the substituents in ligands significantly influenced the activity for ethylene polymerization and molecular weight of resultant polymers as well as the selectivity of 1-hexene. To further investigate the copolymerization system, the reactivity ratios of comonomers were determined using ^{13}C NMR methods of Hsieh and Randall. All vanadium(III) catalysts showed a significantly higher reactivity toward ethylene (r_e = 40–65) as compared to 1-hexene (r_h = 0.01–0.1), and the 1-hexane units should be randomly and homogeneously distributed in the copolymer chains. The steric hindrance and electronic effect of the ligands exert obvious influence on the value of r_e and r_h, which manifested as the copolymerization capability of catalysts. The microstructures and then the mechanism of the chain transfer reaction were also investigated by ^{13}C NMR spectra. The molecular weights of the resultant copolymers decreased sharply with the increase of Al/V molar ratio and the unsaturated end groups were not detected in NMR spectra, indicating that chain-transfer to alkylaluminium was the dominant chain-transfer pathway in the copolymerization.

We believe that the results through this study would introduce important information for designing efficient transition metal catalysts for olefin polymerization.

Experimental

General procedures and materials

All manipulation of air- and/or moisture-sensitive compounds were carried out under a dry argon atmosphere by using standard Schlenk techniques or under a dry argon atmosphere in an MBraun glovebox unless otherwise noted. All solvents were purified from an MBraun SPS system. Commercial ethylene was directly used for polymerization without further purification. NMR of the ligands and vanadium complexes were obtained on a Bruker 300 MHz spectrometer at ambient temperature, with DMSO and $CDCl_3$ as the solvent. The IR spectra were recorded on a Bio-RadFTS-135 spectrophotometer. Elemental analyses were recorded on an elemental Vario EL spectrometer. The ^{13}C NMR data of copolymers were obtained on a Varian Unity-400 MHz spectrometer at 110 °C with *o*-$C_6D_4Cl_2$ as a solvent. The DSC measurements were performed on a Perkin-Elmer Pyris 1 Differential Scanning Calorimeter at a rate of 10 °C min^{-1}. The weight-average molecular weight (M_w) and the polydispersity index (PDI) of polymer samples were determined at 150 °C by a PL-GPC 220 type high-temperature chromatograph equipped with three Plgel 10 μm Mixed-B LS type columns. 1,2,4-Trichlorobenzene (TCB) was employed as the solvent at a flow rate of 1.0 mL min^{-1}. The calibration was made by polystyrene standard EasiCal PS-1 (PL Ltd). Ethyl trichloroacetate (ETA) were purchased from Aldrich, dried over calcium hydride at room temperature and then distilled. $VCl_3(THF)_3$ was purchased from Aldrich. Diethylaluminium chloride was purchased from Albemarle Corporation, triisobutylaluminium, triethylaluminium, trimethylaluminium were purchased from Albemarle Corporation. The other reagents and solvents were commercially available. The ligands used were synthesized according to the literature methods.[17,21]

Synthesis of vanadium complexes

[2,5-C_4H_2N(CH═N-2,6-$iPrC_6H_3$)$_2$]$VCl_2(THF)_2$ (2c). Yield: 76.0%. IR (KBr pellets): ν(C═N) 1566, 1625 cm^{-1}. EI-MS (70 eV): m/z = 705 [M^+]. Anal. calcd for $C_{38}H_{54}Cl_2N_3O_2V$: C, 64.59; H, 7.65; N, 5.95%. Found: C, 64.46; H, 7.59, N, 5.91%.

[2,5-C_4H_2N(CH═N-2,4,6-MeC_6H_2)$_2$]$VCl_2(THF)_2$ (2d). Yield: 70.0%. IR (KBr pellets): ν(C═N) 1569, 1624 cm^{-1}. EI-MS (70 eV): m/z = 621 [M^+]. Anal. calcd for $C_{32}H_{42}Cl_2N_3O_2V$: C, 61.74; H, 6.75; N, 6.75%. Found: C, 61.64; H, 6.69, N, 6.76%.

[2,5-C_4H_2N(CH═NC_6F_5)$_2$]$VCl_2(THF)_2$ (2e). Yield: 56.0%. IR (KBr pellets): ν(C═N) 1569, 1626 cm^{-1}. EI-MS (70 eV): m/z = 717 [M^+]. Anal. calcd for $C_{26}H_{20}Cl_2F_{10}N_3O_2V$: C, 43.45; H, 2.79; N, 5.85%. Found: C, 43.36; H, 2.84, N, 5.91%.

[C_4H_3N(CH═N-2,6-$iPrC_6H_3$)]$_2$VCl(THF) (4f). To a slurry of NaH (0.06 g, 2.5 mmol) in THF (10 mL) was added a solution of ligand **1f** (508 mg, 2.0 mmol) in THF (10 mL) at −30 °C. The resulting suspension was warmed to room temperature and stirred for 4 h. Next, a solution of $VCl_3(THF)_3$ (373 mg, 1.0 mmol) in THF (20 mL) was slowly transferred to the yellow mixture, and the red brown solution was stirred for 12 h. The reaction mixture was condensed and filtered to remove NaCl and the excess NaH. The filtrate was concentrated and recrystallized in THF–n-hexane and yielded 501 mg of the pure complex as a brown solid (75.0%). IR (KBr pellets): ν(C═N) 1624 cm^{-1}. EI-MS (70 eV): m/z = 664 [M^+]. Anal. calcd for $C_{38}H_{50}ClN_4OV$: C, 61.35; H, 7.52; N, 11.01%; Found: C, 61.42; H, 7.53; N, 11.12%.

General procedure for ethylene polymerization. Polymerization was carried out under atmospheric pressure in toluene in a 150 mL glass reactor equipped with a mechanical stirrer. The reactor was charged with 45 mL of toluene, and then the ethylene gas feed was started followed by equilibration at desired polymerization temperature. After 5 min, a solution of Et_2AlCl in toluene and a solution of ETA in toluene were added. Subsequently, a toluene solution of the catalyst was added into the reactor with vigorous stirring (900 rpm) to initiate polymerization. The total volume of the liquid phase was 50 mL. After a prescribed time, alcohol (10 mL) was added to terminate the copolymerization reaction, and the ethylene gas feed was stopped. The resulted mixture was added to acidic alcohol. The solid polymer was isolated by filtration, washed with alcohol and acetone, and dried at 60 °C for 24 h in a vacuum oven.

General procedure for ethylene/1-hexene copolymerization

Copolymerization was carried out under atmospheric pressure in toluene in a 150 mL glass reactor equipped with a mechanical stirrer. The reactor was charged with 30 mL of toluene and the prescribed amount of 1-hexene, and then the ethylene gas feed was started followed by equilibration at desired polymerization temperature. After 5 min, a solution of Et_2AlCl in toluene and a solution of ETA in toluene were added. Subsequently, a toluene solution of catalyst was added into the reactor with vigorous stirring (900 rpm) to initiate copolymerization. The total volume of the liquid phase was 50 mL. After a prescribed time, alcohol (10 mL) was added to terminate the copolymerization reaction, and the ethylene gas feed was stopped. The resulted mixture was added to acidic alcohol. The solid polymer was isolated by filtration,

washed with alcohol and acetone, and dried at 60 °C for 24 h in a vacuum oven.

Crystallographic studies

Crystals for X-ray analysis were obtained as described in the preparations. The crystallographic data, collection parameters, and refinement parameters are listed in Table 1. The crystals were manipulated in a glovebox. The intensity data were collected with the x scan mode (186 K) on a Bruker Smart APEX diffractometer with CCD detector using Mo-Kα radiation (λ = 0.71, 073 E). Lorentz, polarization factors were made for the intensity data and absorption corrections were performed using SADABS program. The crystal structures were solved using the SHELXTL program and refined using full matrix least squares. The positions of hydrogen atoms were calculated theoretically and included in the final cycles of refinement in a riding model along with attached carbons.

DFT calculations

In order to predict the structures of complexes **2a–e**, we employed density functional theory (DFT) calculations for the dissociation energies by using the Amsterdam Density Functional (ADF) program package.[22] The structures and energies are obtained based on the local density approximation augmented with Becke's nonlocal exchange corrections[23] and Perdew's nonlocal correlation correction.[24] A triple STO basis set was employed for V, while all other atoms were described by a double-ζ plus polarization STO basis. The 1s electrons of the C, N and O atoms, as well as the 1s–2p electrons of Cl and V atoms, were treated as frozen core. Finally, first-order scalar relativistic corrections were added to the total energy of the system.

Acknowledgements

The authors are grateful for subsidy provided by the National Natural Science Foundation of China (Nos. 20734002 and 20923003).

References

1 For reviews see: (*a*) S. Gambarotta, *Coord. Chem. Rev.*, 2003, **237**, 229–243; (*b*) H. Hagen, J. Boersma and G. van Koten, *Chem. Soc. Rev.*, 2002, **31**, 357–364; (*c*) L. S. Boffa and B. M. Novak, *Chem. Rev.*, 2000, **100**, 1479–1493; (*d*) C. Redshaw, *Dalton Trans.*, 2010, **39**, 5595–5604; (*e*) K. Nomura and S. Zhang, *Chem. Rev.*, DOI: 10.1021/cr100207h.
2 (*a*) Y. L. Ma, D. Reardon, S. Gambarotta and G. Yap, *Organometallics*, 1999, **18**, 2773–2781; (*b*) D. Reardon, F. Conan, S. Gambarotta, G. Yap and Q. Y. Wang, *J. Am. Chem. Soc.*, 1999, **121**, 9318–9325.
3 (*a*) H. Hagen, C. Bezemer, J. Boersma, H. Kooijman, M. Lutz, A. L. Spek and G. van Koten, *Inorg. Chem.*, 2000, **39**, 3970–3977; (*b*) H. Hagen, J. Boersma, M. Lutz, A. L. Spek and G. van Koten, *Eur. J. Inorg. Chem.*, 2001, 117–123.
4 (*a*) A. K. Tomov, V. C. Gibson, D. Zaher, M. Elsegood and S. H. Dale, *Chem. Commun.*, 2004, 1956–1957; (*b*) C. Redshaw, L. Warford, S. H. Dale and M. R. J. Elsegood, *Chem. Commun.*, 2004, 1954–1955.
5 (*a*) E. Brussee, A. Meetsma, B. Hessen and J. H. Teuben, *Chem. Commun.*, 2000, 497–498; (*b*) E. Brussee, A. Meetsma, B. Hessen and J. H. Teuben, *Organometallics*, 1998, **17**, 4090–4095.
6 (*a*) Z. Janas, L. B. Jerzykiewicz, R. L. Richards and P. Sobota, *Chem. Commun.*, 1999, **11**, 1105–1106; (*b*) Z. Janas, L. B. Jerzykiewicz, S. Przybylak, R. L. Richards and P. Sobota, *Organometallics*, 2000, **19**, 4252–4257; (*c*) Z. Janas, D. Wisniewska, L. B. Jerzykiewicz, P. Sobota, K. Drabent and K. Szczegot, *Dalton Trans.*, 2007, 2065–2069; (*d*) D. Homden, C. Redshaw, L. Warford, D. L. Hughes, J. A. Wright, S. H. Dale and M. R. J. Elsegood, *Dalton Trans.*, 2009, 8900–8910; (*e*) A. Arbaoui, C. Redshaw, D. M. Homden, J. A. Wright and M. R. J. Elsegood, *Dalton Trans.*, 2009, 8911–8922.
7 (*a*) C. Cuomo, S. Milione and A. Grassi, *J. Polym. Sci., Part A: Polym. Chem.*, 2006, **44**, 3279–3289; (*b*) S. Milione, G. Cavallo, C. Tedesco and A. Grassi, *J. Chem. Soc., Dalton Trans.*, 2002, 1839–1846.
8 M. Bialek and O. Liboska, *J. Polym. Sci., Part A: Polym. Chem.*, 2010, **48**, 471–478.
9 (*a*) Y. Nakayama, H. Bando, Y. Sonobe, Y. Suzuki and T. Fujita, *Chem. Lett.*, 2003, **32**, 766–767; (*b*) Y. Nakayama, H. Bando, Y. Sonobe and T. Fujita, *J. Mol. Catal. A:Chem.*, 2004, **213**, 141–150; (*c*) H. Makio, N. Kashiwa and T. Fujita, *Adv. Synth. Catal.*, 2002, **344**, 477–493; (*d*) M. Mitani, T. Nakano and T. Fujita, *Chem.–Eur. J.*, 2003, **9**, 2396–2403.
10 J. Tian, P. D. Hustad and G. W. Coates, *J. Am. Chem. Soc.*, 2001, **123**, 5134–5135.
11 (*a*) V. C. Gibson, S. Mastroianni, C. Newton, C. Redshaw, G. A. Solan, A. J. P. White and D. J. Williams, *J. Chem. Soc., Dalton Trans.*, 2000, 1969–1971; (*b*) D. J. Jones, V. C. Gibson, S. Green and P. J. Maddox, *Chem. Commun.*, 2002, 1038–1039.
12 C. Wang, S. Friedrich, T. R. Younkin, R. T. Li, R. H. Grubbs, D. A. Bansleben and M. W. Day, *Organometallics*, 1998, **17**, 3149–3151.
13 J. Houghton, S. Simonovic, A. C. Whitwood, R. E. Douthwaite, S. A. Carabineiro, J. C. Yuan, M. M. Marques and P. T. Gomes, *J. Organomet. Chem.*, 2008, **693**, 717–724.
14 (*a*) H. Tsurugi, T. Yamagata, K. Tani and K. Mashima, *Chem. Lett.*, 2003, **32**, 756–757; (*b*) H. Tsurugi, Y. Matsuo, T. Yamagata and K. Mashima, *Organometallics*, 2004, **23**, 2797–2805; (*c*) Y. Matsuo, K. Mashima and K. Tani, *Organometallics*, 2001, **20**, 3510–3518.
15 (*a*) V. C. Gibson, P. J. Maddox, C. Newton, C. Redshaw, G. A. Solan, A. J. P. White and D. J. Williams, *Chem. Commun.*, 1998, 1651–1652; (*b*) V. C. Gibson, C. Newton, C. Redshaw, G. A. Solan, A. J. P. White and D. J. Williams, *J. Chem. Soc., Dalton Trans.*, 2002, 4017–4023.
16 (*a*) Y. Yoshida, S. Matsui, Y. Takagi, M. Mitani, T. Nakano, H. Tanaka, N. Kashiwa and T. Fujita, *Organometallics*, 2001, **20**, 4793–4799; (*b*) S. Matsui, T. P. Spaniol, Y. Takagi, Y. Yoshida and J. Okuda, *J. Chem. Soc., Dalton Trans.*, 2002, 4529–4531; (*c*) S. Matsui, Y. Yoshida, Y. Takagi, T. P. Spaniol and J. Okuda, *J. Organomet. Chem.*, 2004, **689**, 1155–1164.
17 D. M. Dawson, D. A. Walker, P. M. Thornton and M. Bochmann, *J. Chem. Soc., Dalton Trans.*, 2000, 459–466.
18 (*a*) L. M. Tang, J. Q. Wu, Y. Q. Duan, L. Pan, Y. G. Li and Y. S. Li, *J. Polym. Sci., Part A: Polym. Chem.*, 2008, **46**, 2038–2048; (*b*) J. Q. Wu, B. X. Li, S. W. Zhang and Y. S. Li, *J. Polym. Sci., Part A: Polym. Chem.*, 2010, **48**, 3062–3072; (*c*) J. Q. Wu, L. Pan, Y. G. Li, S. R. Liu and Y. S. Li, *Organometallics*, 2009, **28**, 1817–1825; (*d*) J. S. Mu, J. Y. Liu, S. R. Liu and Y. S. Li, *Polymer*, 2009, **50**, 5059–5064; (*e*) J. Q. Wu, L. Pan, N. H. Hu and Y. S. Li, *Organometallics*, 2008, **27**, 3840–3848; (*f*) J. Q. Wu, L. Pan, S. R. Liu, L. P. He and Y. S. Li, *J. Polym. Sci., Part A: Polym. Chem.*, 2009, **47**, 3573–3582.
19 B. C. Xu, T. Hu, J. Q. Wu, N. H. Hu and Y. S. Li, *Dalton Trans.*, 2009, 8854–8863.
20 E. T. Hsieh and J. C. Randall, *Macromolecules*, 1982, **15**, 1402–1406.
21 Y. Matsuo, H. Tsurugi, T. Yamagata, K. Tani and K. Mashima, *Bull. Chem. Soc. Jpn.*, 2003, **76**, 1965–1968.
22 (*a*) E. J. Baerends, D. E. Ellis and P. Ros, *Chem. Phys.*, 1973, **2**, 41–51; (*b*) E. J. Baerends and P. Ros, *Chem. Phys.*, 1973, **2**, 52–59; (*c*) G. te Velde and E. J. Baerends, *J. Comput. Phys.*, 1992, **99**, 8498–8503; (*d*) C. G. Fonseca, O. Visser, J. G. Snijders, G. te Velde, E. J. Baerends, in *Methods and Techniques in Computational Chemistry, METECC-95*, E. Clementi, G. Corongiu, ed.; STEF, Cagliari, Italy, 1995, p 305.
23 A. D. Becke, *Phys. Rev. A: At., Mol., Opt. Phys.*, 1988, **38**, 3098–3100.
24 J. P. Perdew, *Phys. Rev. B*, 1986, **33**, 8822–8824.
25 (*a*) D. L. Christman, *J. Polym. Sci., Part A-1*, 1972, **10**, 471; (*b*) H. Hagen, J. Boersma and G. van Koten, *Chem. Soc. Rev.*, 2002, **31**, 357–364.